

HHS Public Access

Author manuscript

Exp Brain Res. Author manuscript; available in PMC 2018 January 01.

Published in final edited form as:

Exp Brain Res. 2017 January; 235(1): 69–81. doi:10.1007/s00221-016-4773-7.

N100 as a generic cortical electrophysiological marker based on decomposition of TMS-evoked potentials across five anatomic locations

Xiaoming Du¹, Fow-Sen Choa², Ann Summerfelt¹, Laura M. Rowland¹, Joshua Chiappelli¹, Peter Kochunov¹, and L. Elliot Hong¹

¹Department of Psychiatry, Maryland Psychiatric Research Center, University of Maryland School of Medicine, P.O. Box 21247, Baltimore, MD 21228, USA

²Department of Electrical Engineering and Computer Science, University of Maryland Baltimore County, Baltimore, MD 21250, USA

Abstract

N100, the negative peak of electrical response occurring around 100 ms, is present in diverse functional paradigms including auditory, visual, somatic, behavioral and cognitive tasks. We hypothesized that the presence of the N100 across different paradigms may be indicative of a more general property of the cerebral cortex regardless of functional or anatomic specificity. To test this hypothesis, we combined transcranial magnetic stimulation (TMS) and electroencephalography (EEG) to measure cortical excitability by TMS across cortical regions without relying on specific sensory, cognitive or behavioral modalities. The five stimulated regions included left prefrontal, left motor, left primary auditory cortices, the vertex and posterior cerebellum with stimulations performed using supra- and subthreshold intensities. EEG responses produced by TMS stimulation at the five locations all generated N100s that peaked at the vertex. The amplitudes of the N100s elicited by these five diverse cortical origins were statistically not significantly different (all uncorrected p > 0.05). No other EEG response components were found to have this global property of N100. Our findings suggest that anatomy- and modality-specific interpretation of N100 should be carefully evaluated, and N100 by TMS may be used as a bio-marker for evaluating local versus general cortical properties across the brain.

Keywords

Transcranial magnetic stimulation; Electroencephalography; N100; Motor cortex; Prefrontal cortex; Cerebellum

Introduction

Event-related potentials (ERPs) are obtained from averaged electroencephalography (EEG) in response to specific sensory input and/or behavioral output events. They provide a

noninvasive approach to study psychophysiological correlates of sensory and/or cognitive processes. Examples of these applications include the use of P50 to measure sensory gating (Olincy and Martin 2005; Vlcek et al. 2014), N200 for assessing spatial attention (Woodman and Luck 2003), N250 as index of familiarity of face (Tanaka et al. 2006) and P300 as a novelty or attention marker (Jeon and Polich 2001; Polich and Comerchero 2003). However, unlike those mentioned components, the N100 component, the negative deflection peak around 100 ms after the onset of stimulus, can be obtained from many if not all tasks in sensory domains. For example, N100 has been found in auditory (van Elk et al. 2014), visual (Mangun and Hillyard 1991), olfactory (Pause et al. 1996), pain (Greffrath et al. 2007), balance (Quant et al. 2005), respiration blocking (Chan and Davenport 2008) and somatosensory paradigms (Wang et al. 2008). Although the N100 effect from each paradigm was usually regarded as specific to that paradigm, the commonality of N100 across them suggests global implications in additional to task-, anatomy- or modality-specific interpretations.

The presence of N100 across diverse stimulation conditions suggests that N100 may be a general feature of the cerebral response to focused activations in addition to its representations of task- and region-specific effects. This hypothesis predicts that N100 can be generated when cortical stimulation is applied in the cortex regardless of specific locations. To test this hypothesis, one needs a way to stimulate discrete cortical regions not relying on specific sensory and behavioral input/output requirements.

The combination of transcranial magnetic stimulation (TMS) and simultaneous EEG provides a means to stimulate and record response from multiple cortical regions without being confined only to sensory or motor areas. Single TMS over motor cortex (M1) can evoke EEG wave forms, currently labeled by many different names including N7, N10, N15, P13, P14, N18, P30, N40, N44, N45, P50, P55, P60, N100, P180 and N280 (Paus et al. 2001; Komssi et al. 2004; Bender et al. 2005; Bonato et al. 2006; Komssi and Kahkonen 2006; Ilmoniemi and Kicic 2010; Maki and Ilmoniemi 2010; Ferreri et al. 2011, 2012; Ter Braack et al. 2015) (more discussion in "Methods"). Among these TMS-evoked components, N100 is the most reproducible component even after removing the TMS soundevoked auditory responses (Bender et al. 2005; Kahkonen and Wilenius 2007; Bonnard et al. 2009; Lioumis et al. 2009). M1 TMS-evoked N100 is thought to reflect intracortical excitatory-inhibitory network activities of the motor cortex pathway (Nikulin et al. 2003; Bender et al. 2005; Kicic et al. 2008). Furthermore, as TMS has been increasingly used to as stimuli in electro-physiology studies, there is a critical need to understand whether N100 and any of these other proposed ERP components are anatomically specific. There is a lack of systematic ERP research based on anatomic distributions of TMS application.

Indeed, TMS has also been applied to several other cortical areas besides M1.TMS to prefrontal cortex reliably evoked N100 (Lioumis et al. 2009). TMS has also been applied to parietal cortex (Johnson et al. 2012) and vertex (Bender et al. 2005) which also yielded robust N100s. However, critical information may be missed on the global nature of the TMS-evoked N100 versus other TMS-evoked ERP components because the relationship of N100s (and other ERP components) across different brain areas was not compared in the same experiment in previous studies. To address this, we applied TMS to five functionally

discrete brain regions. We tested the hypothesis that similar N100 can be generated when TMS stimulations were applied to any of the five locations. We compared the relationship between the N100 responses in 11 distributed electrodes, with the vertex (CZ) being the primary site of interest because N100 has been most commonly measured at this site in ERP studies. Similar comparisons were made for other ERP components, including P200, which was the second largest peak besides N100 in TMS stimulations.

Materials and methods

Participants

Twenty-four healthy volunteers (mean age = 41.9 ± 14.5 years, range 20–62 years; 15 males and 9 females) participated in this study. All subjects were interviewed with the Structured Clinical Interview for DSM-IV to exclude DSM-IV Axis I psychiatric diagnosis. Major medical and neurological illnesses, history of head injury with loss of consciousness, pregnancy and substance dependence within the past 6 months were exclusionary. TMS screening interviews confirmed that none of the subjects had contraindications for TMS (Rossi et al. 2009). All subjects gave their written informed consent approved by the University of Maryland Baltimore Institutional Review Board.

Electromyography recording

Surface electromyography (EMG) was recorded from the right first dorsal interosseous (FDI) muscle with Ag/AgCl disposable electrodes (CareFusion Inc., WI, USA) placed in a tendon–belly montage. The EMG signal was recorded in DC mode with a Neuroscan SynAmps2 amplifier (Charlotte, NC), amplified (gain of 10), digitized at 5000 Hz and stored for offline analysis (Darling et al. 2006). A ground electrode was placed over the right ulnar styloid when EMG alone was recorded. A forehead ground was used when EEG and EMG were recorded simultaneously. Peak-to-peak amplitude of the motor-evoked potentials (MEPs) was measured.

Transcranial magnetic stimulation

TMS was administered over five brain areas separately: left prefrontal cortex (PFC), left motor cortex (M1), left primary auditory cortex (PAC), vertex and posterior cerebellum (vermis), stereotactically localized using the individual's high-resolution structural MRI (Fig. 1). TMS was first applied to left M1 to determine the resting motor threshold (RMT) which was defined according to conventional criteria as the minimum intensity needed to elicit a MEP of >50 μ V in at least 5 out of 10 consecutive stimuli (Rossini et al. 1994; Du et al. 2015). Thereafter, two TMS intensities were tested for each of the five TMS site: suprathreshold (120 % RMT) and subthreshold (80 % RMT). Sham TMS was conducted for each subject by turning the coil 90° and moving away from skull (1–2 cm) while delivering suprathreshold TMS pulses, which preserved the auditory sound of TMS pulses without stimulating any brain regions. Participants wore tight earplugs to muffle the sounds in all conditions. The TMS sounds remained audible in all conditions but were faint. However, because an auditory sound was present, the sham condition was equivalent to an auditory stimulation condition and the recorded ERP was treated as an auditory ERP (Table 1).

The five brain areas were stimulated in 5 sessions, separated by 1 h or more. No more than two sessions were given in the same day. Sham TMS was recorded in the last session. Each participant completed the experiment within 3–10 working days as scheduling permitted. The order of sessions across sites was randomized across participants. Within each session, suprathreshold and subthreshold were delivered in two separate blocks. Within each block, 60 repetitions of the same stimulation were given with jittered inter-stimulation intervals from 4 to 10 s. There were 5- to 10-min breaks between the blocks.

TMS was delivered through a figure-of-eight coil (70 mm outer diameter of each wing) using Magstim 200 Magnetic stimulators with a monophasic current waveform (Magstim Co., Whitland, UK). Prior to the experiment, each subject underwent an anatomic MRI scan (TE/TR/TI = 3.04/2100/785 ms, flip angle = 11° and isotropic spatial resolution of 0.8 mm). The structural images were imported into Brainsight TMS Frameless Navigation system (Rogue Research Inc, Montreal, Canada) to allow for online control of coil positioning (Du et al. 2012, 2014).

For left motor cortex, the stimulus target for each participant was the left cortical area where TMS induced the maximum peak-to-peak motor-evoked potential amplitude from the right FDI muscle (averaged MNI coordinates: -38, -11, 62; same below). The coil was held with the coil handle pointing backward and rotated 45° away from the midline to induce currents that traveled in a posterior-to-anterior direction across the central sulcus (Brasil-Neto et al. 1992; Werhahn et al. 1994; Kammer et al. 2001).

Left prefrontal cortex was defined by the junction of the middle and anterior thirds of the middle frontal gyrus (-39, 33, 37), corresponding to the junction between posterior regions of Brodmann area (BA) 9 and the superior section of BA 46 (Cannon et al. 2005; Farzan et al. 2009). It was also close to F3 electrode in the 10–20 EEG system (Jahanshahi et al. 1998). The coil was held with the coil handle pointing backward.

Vertex was defined as the top of the cerebral cortex (0, -34, 72). The coil handle was pointing backward.

Left primary auditory cortex was defined as superior temporal lobe, corresponding to BA 41 and BA 42 (-62, -38, 10). The coil handle was pointing upward. The participant was sitting in an upright position with chin rest and a mechanical arm supporting head during the TMS stimulations to the above four locations.

Posterior cerebellum was defined as the midpoint of bilateral Crus I/II (0, -79, -26). The participant was positioned in a chin-to-chest flexion position so that the posterior cerebellum was exposed as much as possible. The coil handle was pointing upward (Fig. 1b).

The TMS strengths were calibrated using RMT assessed at the beginning of each session. This is to reduce any potential shifting in cortical sensitivity from session to session. The suprathreshold and subthreshold intensities were always set by the RMT determined before the experiment to each site. However, across the five TMS sites, the intensity for RMT varied little (as seen in "Results").

Electroencephalography recording

EEG was recorded using Neuroscan SynAmps2 (Charlotte, NC) and a specially designed 11 Ag/AgCl sintered electrodes cap for accommodating multi-location TMS and ERP recording. The electrodes were F3, FZ, F4, T3, CZ, T4, P3, PZ, P4, O1 and O2 according to the extended 10–20 system (Fig. 1a). The ground electrode was placed on the forehead and a nose electrode served as a reference. If necessary, the electrode adaptor closest to the TMS site was removed to keep the TMS coil close to the skull; instead a substitute electrode was taped in place as close as possible to the removed electrode position. The locations of the electrodes were digitized with an optical tracking system (Brainsight, Rogue Research Inc., Montreal, Canada). Electrode impedance was kept below 5 kΩ. The amplifier's bandwidth was 0.1–200 Hz with a 60-Hz notch filter, and the signal was sampled at 5000 Hz. Saturation of the EEG amplifiers by the TMS pulse was prevented by using the de-blocking function using a sample-and-hold circuit (e.g., Virtanen et al. 1999; Bonato et al. 2006). The de-blocking started 4 ms before and ended 4 ms after each TMS pulse. The offline analysis was conducted by using Neuroscan 4.3 software and MATLAB (MathWorks, Inc., Natick, MA).

Eyeblink artifacts were minimized using a VEOG-based eyeblink spatial filter routine implemented in Neuroscan software (Semlitsch et al. 1986). In this EOG correction method, the proportion of signals removed from EEG channels is estimated from the eye movement averages which increase the accuracy of EOG correction. Continuous EEG records were epoched from -100 to 500 ms, pre- and post-TMS, respectively, and baseline-corrected and averaged to obtain ERPs. From visual inspections, there were several high-frequency ERP components from 5 to 100 ms, followed by N100 and P200. However, only the N100 and P200 were the regularly present ERP components across 11 electrode sites by 5 TMS sites (Figs. 2, 3). Early TMS-evoked ERP components varied greatly depending on TMS sites and electrode sites, consistent with previous reports of ERP components after TMS to M1 and prefrontal cortex, which have been named N7, N10, N15, P13, P14, N18, P30, N40, N44, N45, P50, P55 and P60 across many studies (Paus et al. 2001; Komssi et al. 2004; Bender et al. 2005; Bonato et al. 2006; Komssi and Kahkonen 2006; Ilmoniemi and Kicic 2010; Maki and Ilmoniemi 2010; Ferreri et al. 2011, 2012; Ter Braack et al. 2015). None of these components consistently appear in all reports, and some of these differently named components may actually belong to the same component (e.g., N40, N44 and N45). These earlier components were considered partially or mainly driven by TMS-related artifacts (Litvak et al. 2007; Veniero et al. 2009; Maki and Ilmoniemi 2010; Mutanen et al. 2013; Rogasch and Fitzgerald 2013). We were unable to identify any early components (before 100 ms) that were consistently identifiable and thus scorable across the 11 electrode sites across the 5 TMS sites in all participants. Therefore, we used only N100 and P200 for subsequent statistical analyses. N100 and P200 were scored from ERPs filtered from 3 to 40 Hz, windowed at 80–180 and 150–280 ms windows, respectively, by an automatic peakdetection algorithm followed by visual inspection blind to conditions. Specifically, for N100, the minimum voltage and its latency within the N100 window (80–180 ms) were marked, while for P200, the maximum voltage and its latency within the P200 window (150-280 ms) were marked. These marked peaks were visually inspected, adjusted if needed and then exported for statistical analysis.

Data analysis

For N100 (and then P200), we first performed repeated-measures ANOVA with 11 electrodes (F3, FZ, F4, T3, CZ, T4, P3, PZ, P4, O1 and O2) and 5 TMS sites (left PFC, left PAC, vertex, left M1 and posterior cerebellum) as within-subject factors on suprathreshold stimulation which elicited larger size of N100 and P200.

As the above analysis confirmed CZ to be the site with the highest amplitudes, we evaluated the TMS intensity effect using only CZ, which is supported by the topographic maps (Fig. 3) and is similar to previous TMS-evoked ERP reports where CZ was also used as the primary site (Spieser et al. 2010; Yamanaka et al. 2013). We conducted a repeated-measure ANOVA at CZ with TMS intensity (supra and subthreshold) and 5 TMS sites as within-subject factors for N100 and then P200.

Next, we compared TMS-induced N100 and TMS sound (from the sham condition)-induced N100 at CZ to identify potential confounds from the TMS click sounds using ANOVA. Greenhouse–Geisser-corrected statistics were reported in all relevant analyses. Paired-sample *t* test was used for post hoc comparisons (two-tailed). False discovery rate (FDR) was used for multiple comparison correction.

To access the auditory contribution to TMS-evoked N100 and P200, the correlations between N100 evoked by suprathreshold TMS at five TMS sties and sham TMS were obtained. However, TMS stimulations not only may induce auditory effects from TMS clicks, but also be able to evoke somatosensory effects from activations of cranial/facial muscles. Mutanen et al. (2013) demonstrated that the TMS-induced muscle activations mainly peak at 4–10 and 8–20 ms. Therefore, we averaged the absolute amplitude of N9, P13, N18 and P25 to represent the TMS-evoked muscle activities and further explored the relationship between these TMS-evoked muscle activities and TMS-evoked N100/P200 by using correlation analysis.

Results

There was no significant difference in the intensity of RMT across the five TMS sites (F(4.0, 92.0) = 1.84, p = 0.13). Temporal and topographic distributions of the earlier (9–60 ms) and later (>70 ms) ERP components were plotted by stimulation site, see Figs. 2 and 3, respectively.

Earlier components

The topographic maps showed that, before 70 ms post-TMS, the response energy distributions were highly variable. They were TMS site specific and no component was seen to consistently peak in the same general location/latency across different stimulation sites (Fig. 2). Many of these components were also present in some but not all participants. Therefore, these earlier components were not subjected to additional statistics.

Later, the globally similar peak activities across TMS sites became apparent around 100 ms and then reappeared around 200 ms, corresponding to the N100 and P200 components; both were prominent at the vertex (CZ) regardless of the TMS site (Fig. 3). However, there were

more variations in the timing of the on and off of the P200 component and its intensity across different TMS sites. The subsequent analyses statistically tested these observations.

N100

The topographic maps showed that suprathreshold TMS-evoked N100 was observed at a temporal window around 130 ms and centered at the vertex (CZ) (Fig. 3 left panels). Repeated-measures ANOVA was used to demonstrate a significant main effect of electrode ((R3.3, 65.4) = 11.35, p < 0.0001) and a significant interaction between electrode and TMS site (R4.4, 87.9) = 4.88, p = 0.001). However, as hypothesized, there was no significant effect of TMS site (R3.1, 62.4) = 0.66, R4 = 0.63), supporting that regardless of locations of TMS application, N100 recorded at CZ was similar in amplitude.

Repeating the statistics in subthreshold TMS across the five TMS sites (tested only at the CZ electrode) as compared with suprathreshold TMS, N100 amplitude showed a significant main effect of intensity (F(1.0, 22.0) = 42.87, p < 0.0001) but not TMS site effect (F(2.6, 57.3) = 1.22, p = 0.31) or TMS site × intensity interaction (F(2.9, 64.9) = 0.32, p = 0.86). The statistics supported that (1) regardless of TMS locations, higher TMS intensity evoked larger N100 at the CZ in an intensity-specific manner such that suprathreshold > subthreshold (Fig. 4) and (2) amplitude of the N100 at the vertex showed no statistical difference across the five TMS sites as long as the TMS intensity was the same.

Finally, between subthreshold and sham, we found that N100 at CZ showed a higher amplitude with subthreshold TMS compared to sham condition at PFC (p = 0.002), M1 (p = 0.01), PAC (p = 0.02) and posterior cerebellum (p = 0.005), but not at vertex (p = 0.79). However, in either TMS intensities, the amplitude of the N100 at the vertex showed no statistical difference across the five TMS sites as long as the TMS intensity was the same.

It is possible that subtle N100 amplitude differences between any two TMS source sites may be present. Therefore, we further compared every two TMS sites using paired-sample t tests, but still found no significant differences between any two sites (all uncorrected ps > 0.05) (Fig. 5c). Therefore, N100 measured at CZ is sensitive to the TMS intensity changes but not to the cortical source of the stimulations.

Finally, there were no significant differences in the latency of the N100 peak at CZ across the TMS sites for suprathreshold or subthreshold TMS (all ps > 0.05).

P200

The topographic maps for each TMS site showed that P200 was elicited mainly at 210 ms and maximally at around the vertex (CZ) as well (Fig. 3, right panels). The amplitude of P200 at CZ also showed a pattern of suprathreshold > sub-threshold (Fig. 4). The repeated-measure ANOVA showed a significant main effect of supra- versus subthreshold intensity (F(1.0, 22.0) = 28.97, p < 0.0001). Unlike N100, P200 showed a significant main effect of TMS site (F(2.2, 48.8) = 3.68, p = 0.03) but not a TMS site × intensity interaction effect (F(2.4, 53.0) = 1.18, P = 0.32). Post hoc tests on the TMS site main effect indicated that P200 evoked by TMS at left PFC (left PFC vs. left M1: P = 0.01; left PFC vs. vertex, P = 0.02) or left PAC (left PAC vs. left M1, P = 0.02; left PAC vs. vertex, P = 0.03) stimulation

was larger than the left M1 and vertex stimulation (Fig. 5d). Therefore, although P200 is also accentuated to CZ regardless of TMS site and is sensitive to TMS strength, it is also significantly marking locations of the cortical stimulation source.

TMS-evoked N100/P200 versus auditory stimulation

We evaluated whether the N100 and P200 components were influenced by auditory stimulation from the TMS sounds. Sham and suprathreshold TMS have identical sound levels. However, suprathreshold TMS stimulation evoked larger N100 than the sham condition at all five TMS sites (all ps < 0.001) (Fig. 5a). Secondly, sham TMS has louder sound level (all sham was delivered at suprathreshold intensity) than subthreshold TMS, but the subthreshold TMS induced a larger N100 than sham condition at most TMS sites (left M1, left PFC, left PAC and posterior cerebellum; all ps < 0.05) except at vertex (p = 0.79). These analyses do not support that the findings were primarily from the TMS sounds.

To access the auditory contribution to TMS-evoked N100, the correlations between N100 evoked by suprathreshold TMS at five TMS sties and sham TMS were obtained. There were only trend-level correlations between sham TMS-evoked N100 and N100 elicited from left PAC stimulation (r= 0.24, p= 0.26), vertex (r= -0.12, p= 0.58), left PFC (r= 0.41, p= 0.05), vermis (r= 0.48, p= 0.017) and left motor cortex (r= 0.36, p= 0.09). None of these trends passed the FDR multiple comparison correction. Furthermore, the TMS-evoked muscle activities, represented by TMS-evoked early components, did not show significant correlation with N100 or P200 (all |r| < 0.40, p > 0.06).

Discussion

N100 is an ERP component that is frequently observed across a wide range of sensory, motor, cognitive, and behavioral tasks. The functional implications of N100 were commonly considered in the context of these specific tasks. Taking advantage of the TMS's ability to stimulate multiple cortical areas not confined by sensory or behavioral modality, the multilocation TMS examination revealed that N100, while not identical, is surprisingly uniform in the location and amplitude of its appearance despite different anatomic activation sources. Based on this finding, we propose that N100 may be an electrophysiological marker of a more general cortical or possibly cortical + subcortical property of the brain, with its mechanism yet to be determined.

While we did not include the right hemisphere or cover cortical areas more densely for reducing burden for research volunteers, we chose stimulation locations that were anatomically diverse (from anterior to the vertex to posterior cerebellum) and functionally distinct (from a higher cognitive function region prefrontal cortex to sensory cortex at PAC to motor cortex at M1). Like sensory stimulus-evoked N100 (Mangun and Hillyard 1991; van Elk et al. 2014), TMS-evoked N100 distributed mainly at vertex and their amplitudes are sensitive to TMS intensity. However, its amplitude at vertex was not significantly changed within subject by stimulating different brain areas as long as the TMS intensity was the same. On the other hand, P200 appeared more amenable to both TMS site effects (Fig. 5). Earlier components before N100 were clearly more variable depending on the TMS stimulation sites and recording locations (Fig. 2).

Single-pulse TMS has been applied to motor, prefrontal and other cortices to elicit ERP components (Bender et al. 2005; Komssi and Kahkonen 2006; Ferreri et al. 2011). The N100 component is robust and well replicated (Komssi et al. 2004; Bender et al. 2005; Bonato et al. 2006; Lioumis et al. 2009). Even in 6- to 10-year-old children, large TMS-evoked N100 was observed (Bender et al. 2005). Paired-pulse TMS can also evoke similar N100 (Premoli et al. 2014b). The TMS-evoked N100 was less studied when TMS was delivered to other brain areas besides M1. Lioumis et al. (2009) found that N100 (component V) was evoked from both left motor and prefrontal cortex stimulation with excellent reproducibility. Johnson et al. (2012) showed an N100 response (based on their Fig. 2b) when single-pulse TMS was delivered over the superior parietal lobule. Also, TMS-evoked N100 was obtained with single vertex stimulation after removing auditory confounds (Ter Braack et al. 2013). However, those N100 evoked by single-pulse TMS over different brain areas were demonstrated separately, and hence, there was no direct comparison between those N100s.

The current study is the first attempt to systematically compare anatomic effect on TMS-evoked ERP components across several discrete locations. By comparing within subject of TMS-evoked components across TMS sites, we found that N100 showed relatively small variation across stimulation sites: no large difference of N100 in terms of its peak location, amplitude and latency was observed between different TMS sites. It is noteworthy that although left PFC, posterior cerebellum and left PAC are relatively far from CZ, TMS over those areas evoked similar N100s as TMS over left M1 and the vertex, which are much closer to CZ. In one TMS/EEG study, Garcia and colleagues used single-pulse TMS to occipital cortex, temporal cortex and vertex with simultaneous EEG and their results demonstrated both site-specific and invariant TMS effects (Garcia et al. 2011). Specifically, they found two time points (116 and 292 ms following the TMS pulse) where the spatial pattern across all their TMS sites was highly similar. The first time point is perfectly in line with the N100 latency (around 120 ms for all TMS sites) in our study.

Each TMS stimulation is accompanied by a TMS-evoked click sound. In the present study, a sham TMS was adopted to represent the TMS-evoked auditory effects. The less amount of N100/P200 elicited by sham TMS and the lack of correlation between TMS-evoked components and sham TMS-evoked components suggest that the TMS sound contributed little to TMS-evoked N100 and P200 components. Besides click sound, TMS stimulation could also induce cranial muscle activities represented by some early ERP components (Mutanen et al. 2013). These muscle-related components were not associated with TMSevoked N100/P200 at all five TMS sites. This supports the idea that the TMS-evoked N100/ P200 was not driven by TMS-evoked muscle activities. However, to fully exclude the explanation of muscle activity, methods thoroughly removing TMS artifacts, such as independent component analysis, are needed (Rogasch et al. 2014). However, the small number of electrodes used here limited the effectiveness of removing artifacts using ICA. For the same reason, cluster-based permutation was not used to directly compare the topographic distribution following stimulation of different brain regions. In the current study, 11 electrodes were used to cover the main cortical regions, which showed that N100 was accentuated at the CZ across all five TMS sites (Fig. 3) among these electrodes. However, this is based on a low-density EEG recording, which limits our ability to fully

interpret the findings in terms of topographic distribution of TMS-evoked components. Future studies with high-density EEG recording will be needed to resolve this issue.

Accompanying each TMS pulse, a tapping sensation could also be evoked by the brief coil vibration (Ilmoniemi and Kicic 2010; Rogasch and Fitzgerald 2013). This tapping sensation may be sufficient to elicit somatosensory-evoked potentials, and such evoked potentials would be expected to occur mainly in the contralateral hemisphere to the site of TMS stimulation. However, in other TMS studies, this asymmetry of somatosensory-evoked potentials was not observed (Paus et al. 2001). Similarly, in the current study, by inspecting the topographic distribution of N100, no apparent hemispheric asymmetry was observed with stimulation of any of the three left-sided TMS sites (left PFC, PAC and M1) (see Fig. 3). Although it is difficult to precisely evaluate the somatosensory contribution to TMSevoked ERP components, previous studies have concluded that they were not a major problem in many TMS studies (Paus et al. 2001; Nikouline et al. 1999; Nikulin et al. 2003; Ilmoniemi and Kicic 2010). However, certain amount of somatosensory contributions may still be possible. Adding a layer of foam between the scalp and coil (Massimini et al. 2005) or adding an extra coil to induce somatosensory sensation for sham TMS (Herring et al. 2015) has been attempted for reducing or controlling the contribution of TMS-evoked somatosensory inputs on final results. In the present study, we introduced a sham condition for TMS-evoked "click" sound, but not for the tapping sensation. Therefore, this potential confound cannot be fully ruled out, although the lack of asymmetry of the N100 distribution in response to left-sided TMS does help to reduce such possibility.

One important limitation of the current study is that the mechanism of TMS-evoked N100 is not clear, impeding our ability to fully interpret the finding. However, some investigators have proposed that TMS-evoked N100 reflects the cortical inhibition induced by TMS (Nikulin et al. 2003; Bender et al. 2005; Kahkonen and Wilenius 2007; Kicic et al. 2008). The amplitude of N100 evoked by TMS to the motor cortex is thought to be modulated by intracortical inhibitory sensorimotor network (Spieser et al. 2010). Inhibition by 1 Hz-rTMS to the motor cortex also reduced the amplitude of single-pulse-evoked N100 (Helfrich et al. 2012). Kahkonen and Wilenius found that alcohol almost abolished TMS-evoked N100 response induced by left motor cortex stimulation, which was interpreted as TMS-evoked N100 being associated with GABA-mediated inhibition (Premoli et al. 2014a; Kahkonen and Wilenius 2007). A recent pharmacological study showed that N100 induced by pairedpulse TMS to the motor cortex was enhanced by a GABA_B receptor agonist (baclofen) and decreased by a positive modulator at GABAA receptor (Premoli et al. 2014a). Evidence from paired-pulse TMS to non-motor cortex such as the dorsolateral prefrontal cortex also supports this opinion (Rogasch et al. 2015). Future pharmacological studies of similar design could extend TMS probes to other cortical areas and test whether the GABAA versus GABA_B effects were a local or global property of the brain using N100 as the readout. Overall, these studies implicated GABA_A, GABA_B and NMDA receptor mechanisms for N100 evoked by TMS to the motor cortex. If the mechanisms are similarly behind the N100 evoked by TMS to the other cortical areas, N100 may provide an interesting electrophysiological biomarker to examine global (rather than local) cortical GABA/NMDA receptor function. Another limitation of the current study is that a uniform stimulation intensity, i.e., 80 % RMT and 120 % RMT, was used across different cortical regions.

Although TMS intensity determined from motor cortex stimulation was widely used in stimulation of non-motor cortex, there is no direct evidence which suggests that same amount of TMS effects occurs in non-motor cortex as in motor cortex. On the other hand, Stokes et al. (2007, 2005, 2013) demonstrated that the TMS effects are highly associated with coil–cortex distance. Given that coil-cortex distance may vary between different TMS sites due to skull and other anatomic structures, the amount of TMS effects reached at different cortical areas may vary. These factors could contribute to the small, non-significant differences in N100 amplitudes across the five TMS sites (see Fig. 5c). However, this is unlikely the reason that we found invariant N100 across five TMS sites, since different amount of TMS stimulation more likely would result in larger differences between TMS sites. However, future studies with TMS intensity adjusted by distance may help to clarify this.

Besides the receptor-level explanation, other possibilities should be considered. For example, the accentuations of the N100 and P200 at the vertex may also suggest that volume conductance or geometric properties of the head may influence the summation of the electric responses to the location. We also considered whether the TMS sounds may have contributed to the effect. However, TMS-induced auditory sound only slightly contributes to the amplitude of N100 and/or P200, since sham TMS with identical suprathreshold click sound generated a much smaller N100 compared to the N100 generated by the TMS pulses. Furthermore, subthreshold TMS pulses induced larger N100 than sham TMS despite the fact that sham TMS had louder sound. Previous studies also showed that earplug or other sound-attenuating methods sharply reduced TMS-evoked N100 (Ter Braack et al. 2015), and the TMS-evoked N100 and P200 were also presented when subject was completely deaf (Ter Braack et al. 2013).

In conclusion, we found that the peak location and amplitude of the TMS-evoked N100 were relatively invariant to TMS sites across widely distributed anatomic locations. This interesting property suggests that N100 is not entirely indexing specific response to particular sensory or behavioral input. Instead, N100 may in part index a more general property of the brain common across diverse origins of cortical activations. This finding illustrates the power of using noninvasive TMS to examine the system-level brain functions. Although the mechanism remains to be determined, the current finding encourages additional mechanistic studies to develop N100 as a potential electro-physiological biomarker for evaluating and modeling the organization of local vs. global cortical activations across the brain.

Acknowledgments

Support was received from NIH grants MH085646, DA027680 and MH103222

References

Bender S, Basseler K, Sebastian I, Resch F, Kammer T, Oelkers-Ax R, Weisbrod M. Electroencephalographic response to transcranial magnetic stimulation in children: evidence for giant inhibitory potentials. Ann Neurol. 2005; 58:58–67. [PubMed: 15984026]

Bonato C, Miniussi C, Rossini PM. Transcranial magnetic stimulation and cortical evoked potentials: a TMS/EEG co-registration study. Clin Neurophysiol. 2006; 117:1699–1707. [PubMed: 16797232]

- Bonnard M, Spieser L, Meziane HB, de Graaf JB, Pailhous J. Prior intention can locally tune inhibitory processes in the primary motor cortex: direct evidence from combined TMS-EEG. Eur J Neurosci. 2009; 30:913–923. [PubMed: 19712104]
- Brasil-Neto JP, McShane LM, Fuhr P, Hallett M, Cohen LG. Topographic mapping of the human motor cortex with magnetic stimulation: factors affecting accuracy and reproducibility. Electroencephalogr Clin Neurophysiol. 1992; 85:9–16. [PubMed: 1371748]
- Cannon TD, Hennah W, van Erp TGM, et al. Association of DISC1/TRAX haplotypes with schizophrenia, reduced prefrontal gray matter, and impaired short-and long-term memory. Arch Gen Psychiatry. 2005; 62:1205–1213. [PubMed: 16275808]
- Chan PY, Davenport PW. Respiratory-related evoked potential measures of respiratory sensory gating. J Appl Physiol. 2008; 105:1106–1113. [PubMed: 18719232]
- Darling WG, Wolf SL, Butler AJ. Variability of motor potentials evoked by transcranial magnetic stimulation depends on muscle activation. Exp Brain Res. 2006; 174:376–385. [PubMed: 16636787]
- Du X, Chen L, Zhou K. The role of the left posterior parietal lobule in top-down modulation on space-based attention: a transcranial magnetic stimulation study. Hum Brain Mapp. 2012; 33:2477–2486. [PubMed: 21922605]
- Du X, Summerfelt A, Chiappelli J, Holcomb HH, Hong LE. Individualized brain inhibition and excitation profile in response to paired-pulse TMS. J Mot Behav. 2014; 46:39–48. [PubMed: 24246068]
- Du X, Choa FS, Summerfelt A, et al. Neural summation in human motor cortex by subthreshold transcranial magnetic stimulations. Exp Brain Res. 2015; 233:671–677. [PubMed: 25399245]
- Farzan F, Barr MS, Wong W, Chen R, Fitzgerald PB, Daskalakis ZJ. Suppression of gamma-oscillations in the dorsolateral prefrontal cortex following long interval cortical inhibition: a TMS-EEG study. Neuropsychopharmacology. 2009; 34:1543–1551. [PubMed: 19037204]
- Ferreri F, Pasqualetti P, Maatta S, et al. Human brain connectivity during single and paired pulse transcranial magnetic stimulation. NeuroImage. 2011; 54:90–102. [PubMed: 20682352]
- Ferreri F, Ponzo D, Hukkanen T, et al. Human brain cortical correlates of short-latency afferent inhibition: a combined EEG-TMS study. J Neurophysiol. 2012; 108:314–323. [PubMed: 22457460]
- Garcia JO, Grossman ED, Srinivasan R. Evoked potentials in large-scale cortical networks elicited by TMS of the visual cortex. J Neurophysiol. 2011; 106:1734–1746. [PubMed: 21715670]
- Greffrath W, Baumgartner U, Treede RD. Peripheral and central components of habituation of heat pain perception and evoked potentials in humans. Pain. 2007; 132:301–311. [PubMed: 17533117]
- Helfrich C, Pierau SS, Freitag CM, Roeper J, Ziemann U, Bender S. Monitoring cortical excitability during repetitive transcranial magnetic stimulation in children with ADHD: a single-blind, sham-controlled TMS-EEG study. PLoS ONE. 2012; 7:e50073. [PubMed: 23185537]
- Herring JD, Thut G, Jensen O, Bergmann TO. Attention modulates TMS-locked alpha oscillations in the visual cortex. J Neurosci. 2015; 35:14435–14447. [PubMed: 26511236]
- Ilmoniemi RJ, Kicic D. Methodology for combined TMS and EEG. Brain Topogr. 2010; 22:233–248. [PubMed: 20012350]
- Jahanshahi M, Profice P, Brown RG, Ridding MC, Dirnberger G, Rothwell JC. The effects of transcranial magnetic stimulation over the dorsolateral prefrontal cortex on suppression of habitual counting during random number generation. Brain. 1998; 121(Pt 8):1533–1544. [PubMed: 9712014]
- Jeon YW, Polich J. P3a from a passive visual stimulus task. Clin Neurophysiol. 2001; 112:2202–2208. [PubMed: 11738190]
- Johnson JS, Kundu B, Casali AG, Postle BR. Task-dependent changes in cortical excitability and effective connectivity: a combined TMS-EEG study. J Neurophysiol. 2012; 107:2383–2392. [PubMed: 22323626]
- Kahkonen S, Wilenius J. Effects of alcohol on TMS-evoked N100 responses. J Neurosci Methods. 2007; 166:104–108. [PubMed: 17727957]

Kammer T, Beck S, Thielscher A, Laubis-Herrmann U, Topka H. Motor thresholds in humans: a transcranial magnetic stimulation study comparing different pulse waveforms, current directions and stimulator types. Clin Neurophysiol. 2001; 112:250–258. [PubMed: 11165526]

- Kicic D, Lioumis P, Ilmoniemi RJ, Nikulin VV. Bilateral changes in excitability of sensorimotor cortices during unilateral movement: combined electroencephalographic and transcranial magnetic stimulation study. Neuroscience. 2008; 152:1119–1129. [PubMed: 18353562]
- Komssi S, Kahkonen S. The novelty value of the combined use of electroencephalography and transcranial magnetic stimulation for neuroscience research. Brain Res Rev. 2006; 52:183–192. [PubMed: 16545462]
- Komssi S, Kahkonen S, Ilmoniemi RJ. The effect of stimulus intensity on brain responses evoked by transcranial magnetic stimulation. Hum Brain Mapp. 2004; 21:154–164. [PubMed: 14755835]
- Lioumis P, Kicic D, Savolainen P, Makela JP, Kahkonen S. Reproducibility of TMS-Evoked EEG responses. Hum Brain Mapp. 2009; 30:1387–1396. [PubMed: 18537115]
- Litvak V, Komssi S, Scherg M, et al. Artifact correction and source analysis of early electroencephalographic responses evoked by transcranial magnetic stimulation over primary motor cortex. NeuroImage. 2007; 37:56–70. [PubMed: 17574872]
- Maki H, Ilmoniemi RJ. The relationship between peripheral and early cortical activation induced by transcranial magnetic stimulation. Neurosci Lett. 2010; 478:24–28. [PubMed: 20435086]
- Mangun GR, Hillyard SA. Modulations of sensory-evoked brain potentials indicate changes in perceptual processing during visual-spatial priming. J Exp Psychol Hum Percept Perform. 1991; 17:1057–1074. [PubMed: 1837297]
- Massimini M, Ferrarelli F, Huber R, Esser SK, Singh H, Tononi G. Breakdown of cortical effective connectivity during sleep. Science (New York, NY). 2005; 309:2228–2232.
- Mutanen T, Maki H, Ilmoniemi RJ. The effect of stimulus parameters on TMS-EEG muscle artifacts. Brain Stimul. 2013; 6:371–376. [PubMed: 22902312]
- Nikouline V, Ruohonen J, Ilmoniemi RJ. The role of the coil click in TMS assessed with simultaneous EEG. Clin Neurophysiol. 1999; 110:1325–1328. [PubMed: 10454266]
- Nikulin VV, Kicic D, Kahkonen S, Ilmoniemi RJ. Modulation of electroencephalographic responses to transcranial magnetic stimulation: evidence for changes in cortical excitability related to movement. Eur J Neurosci. 2003; 18:1206–1212. [PubMed: 12956719]
- Olincy A, Martin L. Diminished suppression of the P50 auditory evoked potential in bipolar disorder subjects with a history of psychosis. Am J Psychiatry. 2005; 162:43–49. [PubMed: 15625200]
- Paus T, Sipila PK, Strafella AP. Synchronization of neuronal activity in the human primary motor cortex by transcranial magnetic stimulation: an EEG study. J Neurophysiol. 2001; 86:1983–1990. [PubMed: 11600655]
- Pause BM, Sojka B, Krauel K, Ferstl R. The nature of the late positive complex within the olfactory event-related potential (OERP). Psychophysiology. 1996; 33:376–384. [PubMed: 8753937]
- Polich J, Comerchero MD. P3a from visual stimuli: typicality, task, and topography. Brain Topogr. 2003; 15:141–152. [PubMed: 12705810]
- Premoli I, Castellanos N, Rivolta D, et al. TMS-EEG signatures of GABAergic neurotransmission in the human cortex. J Neurosci. 2014a; 34:5603–5612. [PubMed: 24741050]
- Premoli I, Rivolta D, Espenhahn S, Castellanos N, Belardinelli P, Ziemann U, Muller-Dahlhaus F. Characterization of GABAB-receptor mediated neurotransmission in the human cortex by paired-pulse TMS-EEG. NeuroImage. 2014b; 103C:152–162.
- Quant S, Maki BE, McIlroy WE. The association between later cortical potentials and later phases of postural reactions evoked by perturbations to upright stance. Neurosci Lett. 2005; 381:269–274. [PubMed: 15896482]
- Rogasch NC, Fitzgerald PB. Assessing cortical network properties using TMS-EEG. Hum Brain Mapp. 2013; 34:1652–1669. [PubMed: 22378543]
- Rogasch NC, Thomson RH, Farzan F, et al. Removing artefacts from TMS-EEG recordings using independent component analysis: importance for assessing prefrontal and motor cortex network properties. Neuroimage. 2014; 101:425–439. [PubMed: 25067813]

Rogasch NC, Daskalakis ZJ, Fitzgerald PB. Cortical inhibition of distinct mechanisms in the dorsolateral prefrontal cortex is related to working memory performance: a TMS-EEG study. Cortex. 2015; 64:68–77. [PubMed: 25461708]

- Rossi S, Hallett M, Rossini PM, Pascual-Leone A. Safety, ethical considerations, and application guidelines for the use of transcranial magnetic stimulation in clinical practice and research. Clin Neurophysiol. 2009; 120:2008–2039. [PubMed: 19833552]
- Rossini PM, Barker AT, Berardelli A, et al. Non-invasive electrical and magnetic stimulation of the brain, spinal cord and roots: basic principles and procedures for routine clinical application. Report of an IFCN committee. Electroencephalogr Clin Neurophysiol. 1994; 91:79–92. [PubMed: 7519144]
- Semlitsch HV, Anderer P, Schuster P, Presslich O. A solution for reliable and valid reduction of ocular artifacts, applied to the P300 ERP. Psychophysiology. 1986; 23:695–703. [PubMed: 3823345]
- Spieser L, Meziane HB, Bonnard M. Cortical mechanisms underlying stretch reflex adaptation to intention: a combined EEG-TMS study. Neuroimage. 2010; 52:316–325. [PubMed: 20398768]
- Stokes MG, Chambers CD, Gould IC, Henderson TR, Janko NE, Allen NB, Mattingley JB. Simple metric for scaling motor threshold based on scalp-cortex distance: application to studies using transcranial magnetic stimulation. J Neurophysiol. 2005; 94:4520–4527. [PubMed: 16135552]
- Stokes MG, Chambers CD, Gould IC, English T, McNaught E, McDonald O, Mattingley JB. Distance-adjusted motor threshold for transcranial magnetic stimulation. Clin Neurophysiol. 2007; 118:1617–1625. [PubMed: 17524764]
- Stokes MG, Barker AT, Dervinis M, Verbruggen F, Maizey L, Adams RC, Chambers CD. Biophysical determinants of transcranial magnetic stimulation: effects of excitability and depth of targeted area. J Neurophysiol. 2013; 109:437–444. [PubMed: 23114213]
- Tanaka JW, Curran T, Porterfield AL, Collins D. Activation of preexisting and acquired face representations: the N250 event-related potential as an index of face familiarity. J Cogn Neurosci. 2006; 18:1488–1497. [PubMed: 16989550]
- Ter Braack EM, de Jonge B, van Putten MJ. Reduction of TMS induced artifacts in EEG using principal component analysis. IEEE Trans Neural Syst Rehabil Eng. 2013; 21:376–382. [PubMed: 23359012]
- Ter Braack EM, de Vos CC, van Putten MJ. Masking the auditory evoked potential in TMS-EEG: a comparison of various methods. Brain Topogr. 2015; 28:520–528. [PubMed: 23996091]
- van Elk M, Salomon R, Kannape O, Blanke O. Suppression of the N1 auditory evoked potential for sounds generated by the upper and lower limbs. Biol Psychol. 2014; 102:108–117. [PubMed: 25019590]
- Veniero D, Bortoletto M, Miniussi C. TMS-EEG co-registration: on TMS-induced artifact. Clin Neurophysiol. 2009; 120:1392–1399. [PubMed: 19535291]
- Virtanen J, Ruohonen J, Naatanen R, Ilmoniemi RJ. Instrumentation for the measurement of electric brain responses to transcranial magnetic stimulation. Med Biol Eng Comput. 1999; 37:322–326. [PubMed: 10505382]
- Vlcek P, Bob P, Raboch J. Sensory disturbances, inhibitory deficits, and the P50 wave in schizophrenia. Neuropsychiatr Dis Treat. 2014; 10:1309–1315. [PubMed: 25075189]
- Wang AL, Mouraux A, Liang M, Iannetti GD. The enhancement of the N1 wave elicited by sensory stimuli presented at very short inter-stimulus intervals is a general feature across sensory systems. PLoS ONE. 2008; 3:e3929. [PubMed: 19081790]
- Werhahn KJ, Fong JK, Meyer BU, Priori A, Rothwell JC, Day BL, Thompson PD. The effect of magnetic coil orientation on the latency of surface EMG and single motor unit responses in the first dorsal interosseous muscle. Electroencephalogr Clin Neurophysiol. 1994; 93:138–146. [PubMed: 7512920]
- Woodman GF, Luck SJ. Serial deployment of attention during visual search. Journal of experimental psychology Hum Percept Perform. 2003; 29:121–138.
- Yamanaka K, Kadota H, Nozaki D. Long-latency TMS-evoked potentials during motor execution and inhibition. Front Hum Neurosci. 2013; 7:751. [PubMed: 24282400]

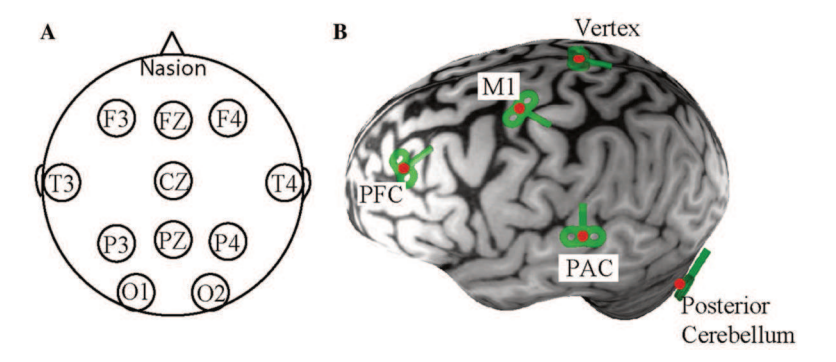


Fig. 1. Illustration of electrode montage and TMS sites. a Illustration of electrodes montage. b Five TMS stimulation positions [left prefrontal cortex (PFC), left motor cortex (M1), left primary auditory cortex (PAC), vertex and posterior cerebellum (vermis)] are showed in a 3D brain of one subject. *Red dots* indicate TMS-targeted cortical areas; *green coils* indicate TMS coil positions and orientations (color figure online)

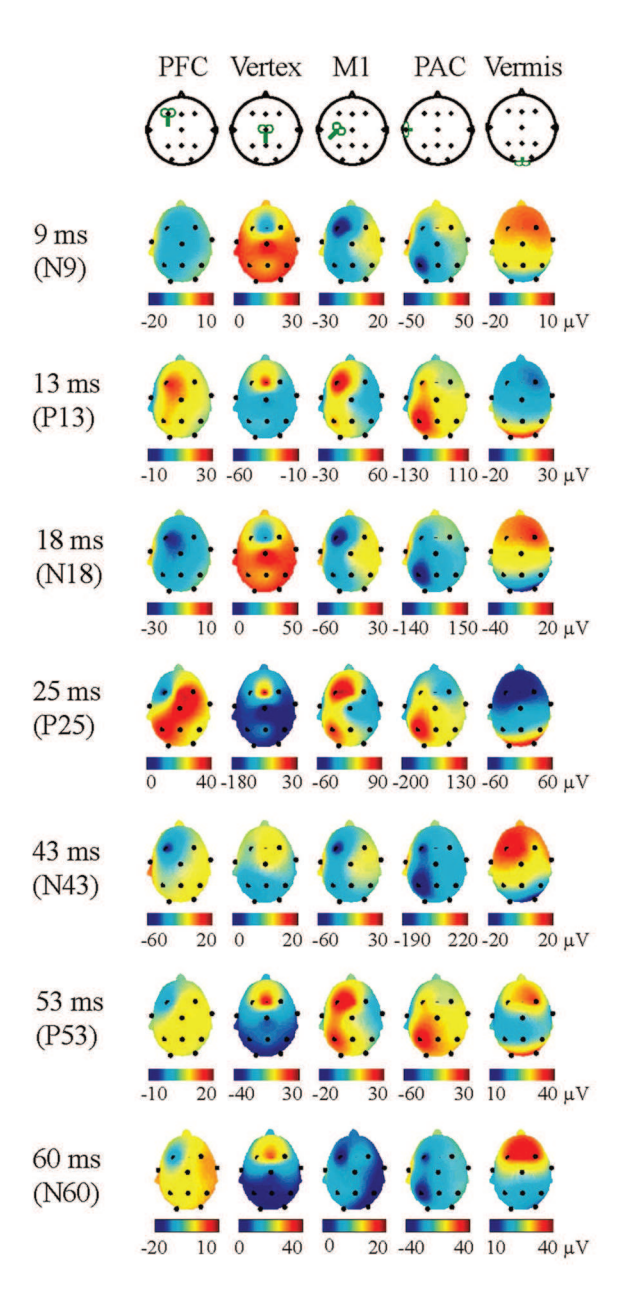


Fig. 2. Topographic evolution maps of TMS-evoked early ERP components (9–60 ms post-stimulus). Maps reflect times where several commonly referred TMS-evoked components were named (N9, N18, P25, N43 and N60). Across the five TMS sites (*left*-to-*right* graph columns), and across N9 to N60 ERP components, there was no component that was accentuated to the same general location and latency across all five stimulation sites. For example, at 43 ms post-stimulus where the so-called N43 component is suppose to appear as reported in previous studies, one cannot observe a negatively peak polarity present in a scalp location consistent across the five stimulation sites, suggesting that these other early components are stimulation site specific and were highly affected by artifacts such as TMS-

evoked muscle activity and thus associated with large variability in maximum/minimum amplitudes from one TMS site to the other

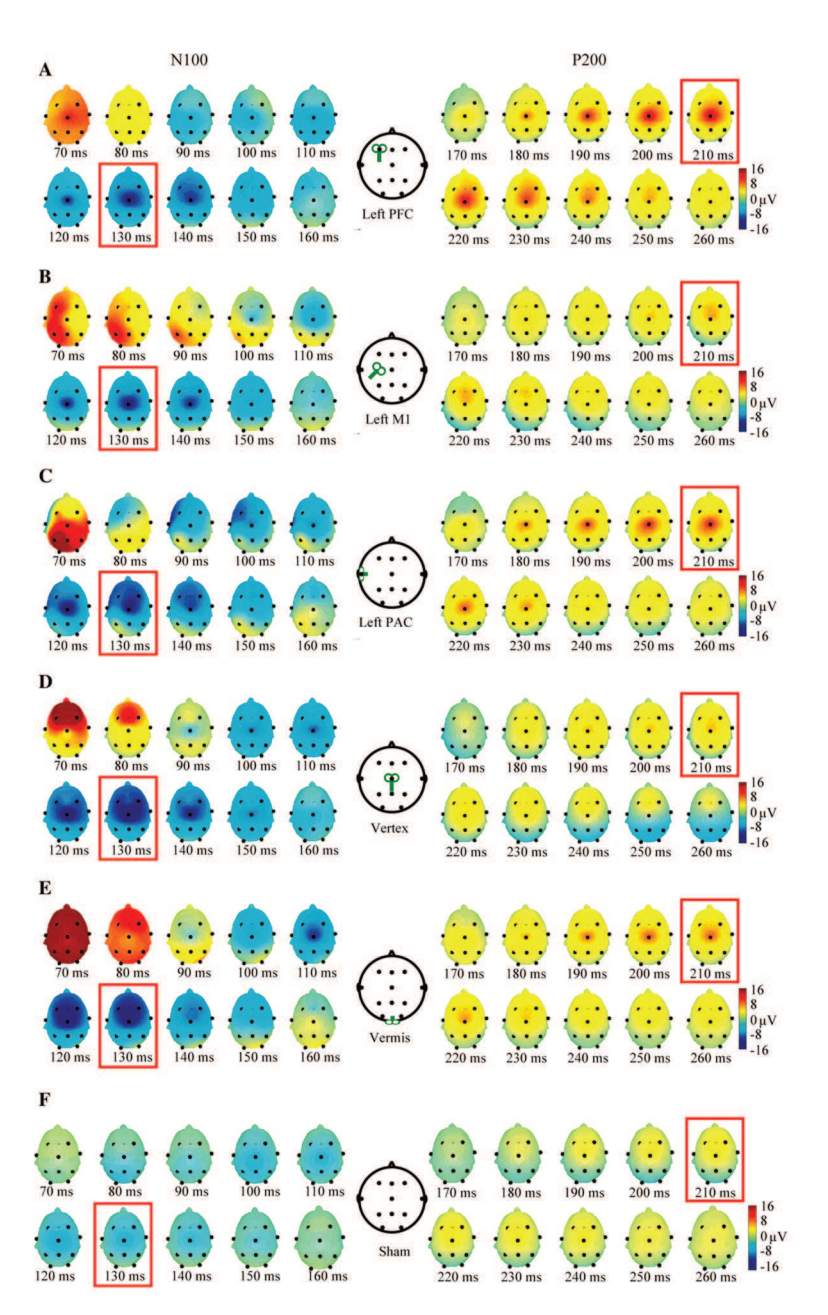


Fig. 3.
Topographic evolution maps of TMS-evoked N100 and P200 ERP (70–260 ms post-stimulus). The distributions of TMS-evoked potentials from 70 to 160 ms with 10 ms step are shown on the *left*: the negative peak (N100) occurred mainly at 130 ms and around vertex (CZ). The topographic maps of TMS-evoked potentials from 170 to 260 ms are shown on the *right*: the positive peak (P200) appeared at around 210 ms and vertex (CZ). The topographic maps at 130 ms for N100 and 210 ms for P200 are highlighted with *red frames*. The electrode montage and TMS coil position are shown in the *middle*. The peak N100 and P200 converged at or around the vertex (CZ) site irrespective of the stimulation site (color figure online)

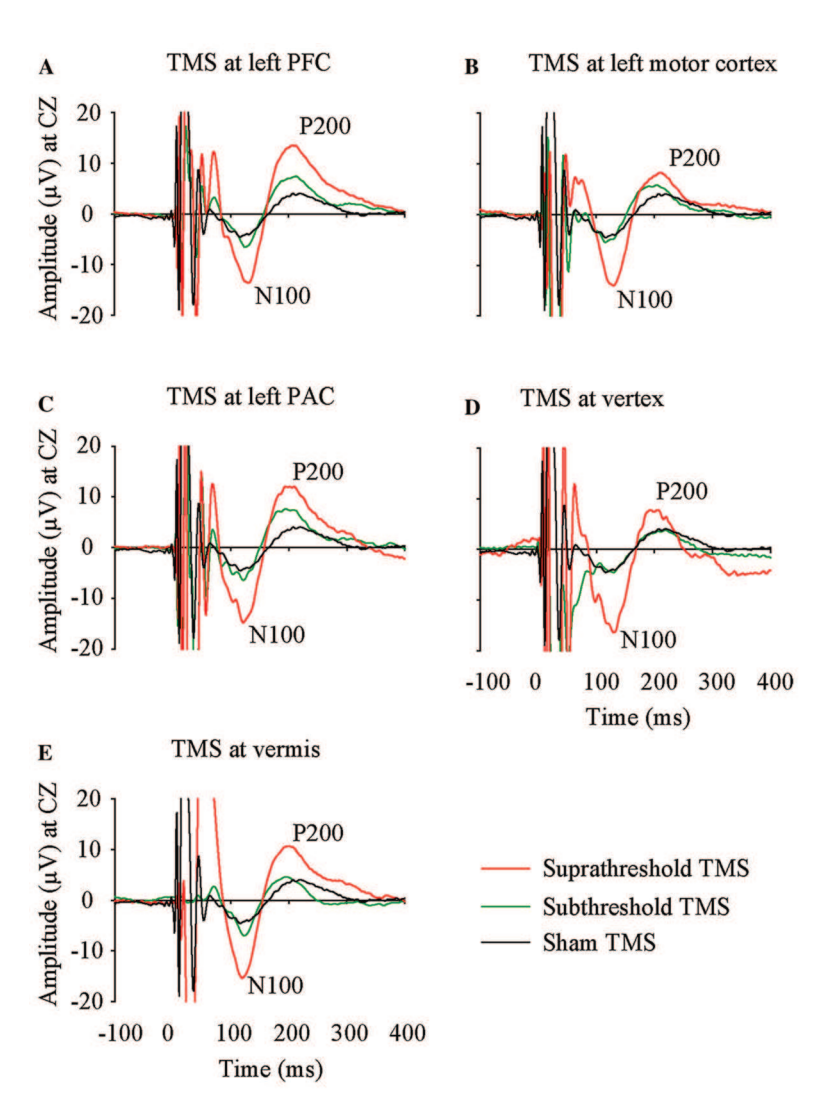


Fig. 4. Grand average of multi-location evoked AEP components recorded at electrode CZ. **a**–**e** are the five TMS sites. Note the nearly identical peak amplitude of N100 at CZ in response to TMS across the five different activation locations

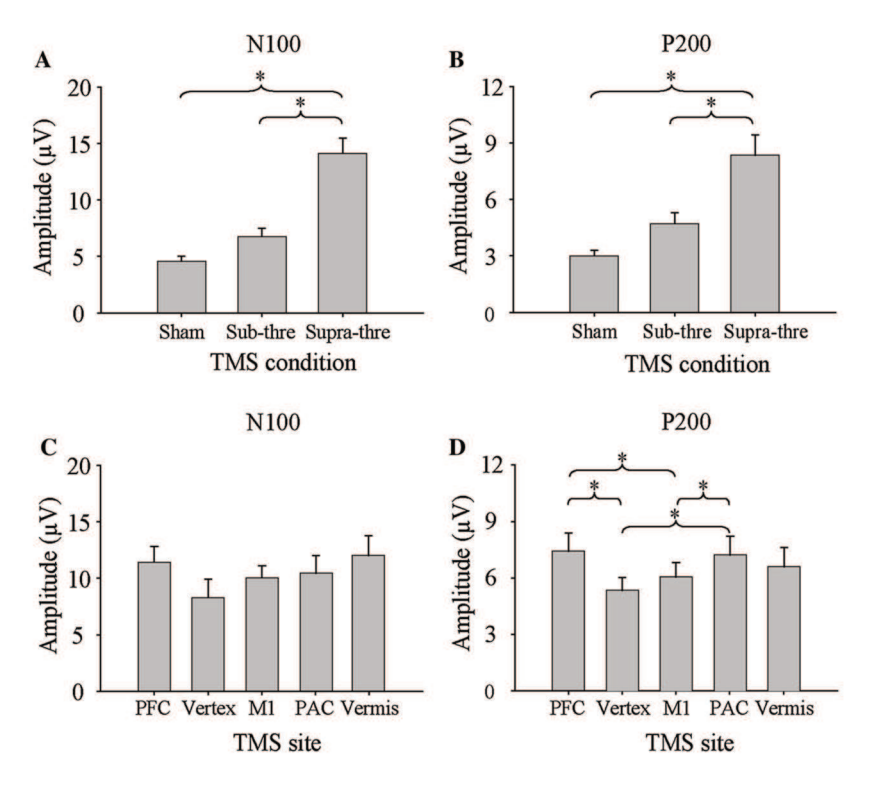


Fig. 5. N100 and P200 at CZ across TMS sites and intensities. **a**, **b** Grand averages (of five TMS sites) of amplitudes of N100 and P200 at CZ electrode under different TMS intensities are shown (mean and SE). Larger amplitude of N100 and P200 was evoked by higher TMS intensity. **c**, **d** Grand averages of N100 and P200 at CZ evoked by different TMS sites at suprathreshold intensity. No statistically significant difference of the N100 amplitude at CZ evoked by TMS from different sites. For P200, stimulation over left PFC and left PAC induced larger P200 than TMS over M1 or vertex. "Asterisk" indicates uncorrected p < 0.05; "Sub-thre" stands for subthreshold TMS; "Supra-thre" stands for suprathreshold TMS

Table 1

Amplitude and latency of potentials evoked by suprathreshold TMS or sham TMS (mean \pm SD). (Note that because of the individualized latencies, the amplitudes here are slightly different from amplitudes shown from grand average)

	PFC	Vertex	M1	PAC	Vermis	Sham
N100	$-15\pm 9~\mu V$	$-12 \pm 11 \; \mu V$	$-14 \pm 7 \mu V$	$-13 \pm 12 \mu\text{V}$	$-16 \pm 13 \mu V$	$-5 \pm 2 \mu V$
	$124 \pm 20 \text{ ms}$	$146 \pm 40 \text{ ms}$	$136 \pm 29 \text{ ms}$	$127 \pm 22 \text{ ms}$	$117 \pm 16 \text{ ms}$	$124 \pm 17 \text{ ms}$
P200	$10 \pm 6 \mu V$	$7 \pm 6 \mu V$	$8 \pm 5 \ \mu V$	$9 \pm 7 \mu V$	$8 \pm 6 \mu V$	$3 \pm 1 \mu\text{V}$
	$199 \pm 19 \text{ ms}$	$225 \pm 72 \text{ ms}$	$201 \pm 33 \text{ ms}$	$194 \pm 18 \text{ ms}$	$196 \pm 23 \text{ ms}$	$204 \pm 21 \text{ ms}$